ISSN 1001-0742
CN 11-2629/X

2012
Volume 24
Number 6

JOURNAL OF ENVIRONMENTAL SCIENCES

Sponsored by
Research Center for Eco-Environmental Sciences
Chinese Academy of Sciences

ELSEVIER
Science Press

JOURNAL OF ENVIRONMENTAL SCIENCES

(http://www.jesc.ac.cn)

Aims and scope

Journal of Environmental Sciences is an international academic journal supervised by Research Center for Eco-Environmental Sciences, Chinese Academy of Sciences. The journal publishes original, peer-reviewed innovative research and valuable findings in environmental sciences. The types of articles published are research article, critical review, rapid communications, and special issues.

The scope of the journal embraces the treatment processes for natural groundwater, municipal, agricultural and industrial water and wastewaters; physical and chemical methods for limitation of pollutants emission into the atmospheric environment; chemical and biological and phytoremediation of contaminated soil; fate and transport of pollutants in environments; toxicological effects of terrorist chemical release on the natural environment and human health; development of environmental catalysts and materials.

For subscription to electronic edition

Elsevier is responsible for subscription of the journal. Please subscribe to the journal via http://www.elsevier.com/locate/jes.

For subscription to print edition

China: Please contact the customer service, Science Press, 16 Donghuangchenggen North Street, Beijing 100717, China. Tel: +86-10-64017032; E-mail: journal@mail.sciencep.com, or the local post office throughout China (domestic postcode: 2-580).

Outside China: Please order the journal from the Elsevier Customer Service Department at the Regional Sales Office nearest you.

Submission declaration

Submission of an article implies that the work described has not been published previously (except in the form of an abstract or as part of a published lecture or academic thesis), that it is not under consideration for publication elsewhere. The submission should be approved by all authors and tacitly or explicitly by the responsible authorities where the work was carried out. If the manuscript accepted, it will not be published elsewhere in the same form, in English or in any other language, including electronically without the written consent of the copyright-holder.

Submission declaration

Submission of the work described has not been published previously (except in the form of an abstract or as part of a published lecture or academic thesis), that it is not under consideration for publication elsewhere. The publication should be approved by all authors and tacitly or explicitly by the responsible authorities where the work was carried out. If the manuscript accepted, it will not be published elsewhere in the same form, in English or in any other language, including electronically without the written consent of the copyright-holder.

Editorial

Authors should submit manuscript online at http://www.jesc.ac.cn. In case of queries, please contact editorial office, Tel: +86-10-62920553, E-mail: jesc@263.net, jesc@rcees.ac.cn. Instruction to authors is available at http://www.jesc.ac.cn.

Copyright

ISSN 1001–0742 **Journal of Environmental Sciences** Vol. 24 No. 6 2012

CONTENTS

Aquatic environment

Terrestrial environment

Environmental biology

Environmental health and toxicology

Environmental catalysis and materials

Serial parameter: CN 11-2629/X*1989*m*188*en*P*22*2012-6

Available online at www.sciencedirect.com
ScienceDirect
Journal of Environmental Sciences 2012, 24(6) 979–989

JOURNAL OF ENVIRONMENTAL SCIENCES
ISSN 1001-0742
CN 11-2629/X
www.jesc.ac.cn

Hydrogeochemical and mineralogical characteristics related to heavy metal attenuation in a stream polluted by acid mine drainage: A case study in Dabaoshan Mine, China

Huarong Zhao[1,2], Beicheng Xia[1,*], Jianqiao Qin[3], Jiaying Zhang[1]

1. School of Environmental Science and Engineering, Sun Yat-Sen University, Guangzhou 510275, China. E-mail: xiabch@mail.sysu.edu.cn
2. School of Environmental Science and Engineering, Guilin University of Technology, Guilin 541004, China
3. Guangdong Provincial Academy of Environmental Science, Guangzhou 510045, China

Received 27 July 2011; revised 18 September 2011; accepted 01 November 2011

Abstract

Dabaoshan Mine, the largest mine in south China, has been developed since the 1970s. Acid mine drainage (AMD) discharged from the mine has caused severe environmental pollution and human health problems. In this article, chemical characteristics, mineralogy of ocher precipitations and heavy metal attenuation in the AMD are discussed based on physicochemical analysis, mineral analysis, sequential extraction experiments and hydrogeochemistry. The AMD chemical characteristics were determined from the initial water composition, water-rock interactions and dissolved sulfide minerals in the mine tailings. The waters, affected and unaffected by AMD, were Ca-SO_4 and Ca-HCO_3 types, respectively. The affected water had a low pH, high SO_4^{2-} and high heavy metal content and oxidation as determined by the Fe^{2+}/Fe^{3+} couple. Heavy metal and SO_4^{2-} contents of Hengshi River water decreased, while pH increased, downstream. Schwertmannite was the major mineral at the waste dump, while goethite and quartz were dominant at the tailings dam and streambed. Schwertmannite was transformed into goethite at the tailings dam and streambed. The sulfate ions of the secondary minerals changed from bidentate- to monodentate-complexes downstream. Fe-Mn oxide phases of Zn, Cd and Pb in sediments increased downstream. However, organic matter complexes of Cu in sediments increased further away from the tailings. Fe^{3+} mineral precipitates and transformations controlled the AMD water chemistry.

Key words: acid mine drainage; Dabaoshan Mine; heavy metal attenuation; hydrogeochemical; PHREEQC

DOI: 10.1016/S1001-0742(11)60868-1

Introduction

The oxidation of sulfide minerals (e.g., pyrite) to produce acid mine drainage (AMD) at mine sites has been widely studied (Task, 1989) because AMD with high levels of sulfate and heavy metals at low pH (Mylona et al., 2000) decreases the biodiversity of water-ecosystems (Sydnor and Redente, 2002; Tordoff et al., 2000), contaminates the soil and plants, and endangers human health.

Dabaoshan Mine, the largest mine in south China, has been extensively mined since the 1970s, with massive tailings left behind and the surroundings have borne the effects of AMD contamination (Liu et al., 2009; Zhou et al., 2007). Production of AMD continues in the tailings reservoir (Bao et al., 2009; Lin et al., 2005b).

Contamination from Dabaoshan Mine has been of concern since cadmium pollution occurred in the Beijiang River (the main tributary of the Pearl River) in December 2005. The local government and the Dabaoshan Mining Corporation Limited have taken measures to reduce the impacts of the AMD. These measures include reinforcing the tailings reservoir, the revegetation of waste mining land and AMD treatment, but the problem still exists. The literature reports that low pH, high-level heavy metal content and intense rainfall were the main reasons for the ineffectiveness of the measures (Sánchez-España et al., 2005).

Most research groups have focused on the environmental impact of AMD in this area, especially soil, water and plant contamination (Li et al., 2009; Lin et al., 2005a, 2005b; Liu et al., 2009; Zhou et al., 2007), toxicity to aquatic life (Chen et al., 2007; Lin et al., 2007), human health assessment of the residents (Bao et al., 2009; Zhuang et al., 2009a, 2009b) and the magnetic characteristics of contaminated soils (Zhou and Xia, 2010). However, they neglected to discuss the hydrogeochemical and secondary mineral characteristics of the waters affected by AMD, such as water chemical composition, secondary mineral transformations and heavy metal natural attenuation in the AMD. These characteristics are important not only for establishing the solution chemistry of the AMD but also for environmental remediation.

The environmental problems in the vicinity of the mine

* Corresponding author: E-mail: xiabch@mail.sysu.edu.cn

are mainly caused by AMD pollution (Wu et al., 2009). The high levels of heavy metals are toxic to both aquatic life and terrestrial plants. Low pH values may damage the environmental enzymatic systems and decrease the respiratory action of plants. Removal of the heavy metals and raising the pH value of AMD-affected water are essential for environmental remediation. Secondary minerals (such as, Fe, Al and Mn oxyhydroxides) adsorb the heavy metals in AMD and the sorption process is essential for heavy metal attenuation in AMD (Bigham et al., 1996b; Fukushi et al., 2003; Kumpulainen et al., 2007; Munk et al., 2002; Ranville et al., 2004; Sánchez-España et al., 2005, 2006; Wu et al., 2009).

The sulfide tailings are classified into arkosite-type, carbonate-type, siliceous-type and silicate-type according to the gangue minerals. AMD produced by carbonate-type tailings are ignored based on the knowledge that limestone reacts with sulfide minerals and buffers the AMD. The processes are described by the following reactions (Holmström et al., 1999):

$$FeS_2 + 3.75O_2 + 3.5H_2O + 4CaCO_3 \longrightarrow Fe(OH)_3 + 4HCO_3^- + 2SO_4^{2+} + 4Ca^{2+} \quad (1)$$

$$Fe_{1-x}S + (9\text{-}3x)/4O_2 + (5\text{-}3x)/2H_2O + 2xCaCO_3 \longrightarrow (1\text{-}x)Fe(OH)_3 + 2(1\text{-}x)H^+ + SO_4^{2+} + 2xCa^{2+} + 2xHCO_3^- \quad (2)$$

where, x is in the range of 0–0.125.

However, AMD generated from carbonate-type tailings have been observed (Morin and Hutt, 1997). An armor is formed as the carbonate minerals coat the secondary mineral precipitates, biofilms and bacteria, and the ratios of Reactions (1) and (2) decrease (Robbins et al., 1999). Therefore, the hydrogeochemical and secondary mineral characteristics of carbonate-type tailings are essential for understanding the AMD polluted areas.

The average contents of CaO and MgO of Dabaoshan Mine were 7.82 wt.% (n = 26) and 3.58 wt.% (n = 26), respectively (Ge and Han, 1987). The tailings belong to the carbonate-type. However, a high level of heavy metal concentrations was determined in the Hengshi River, which is a tributary of the Beijiang River. Moreover, the Beijiang River is a primary water resource of Guangzhou. Therefore, to investigate the migration, transformation and attenuation of heavy metal in the Hengshi River is important both for water resource management and for AMD theory. To discuss the hydrogeochemical and secondary mineral characteristics and heavy metal attenuation of AMD in the vicinity of the Dabaoshan Mine, the following topics were investigated: (1) the physicochemical characteristics of the affected water; (2) the mineralogy of the ocher precipitates; and (3) natural heavy metal attenuation of AMD.

1 Materials and methods

1.1 Location and geological setting

Dabaoshan Mine (24°34′28″N, 113°43′42″E) (Fig. 1) is located in the north of Guangdong Province, south China. It has a subtropical humid monsoon climate. The average annual temperature is 20°C and rainfall is 1800 mm.

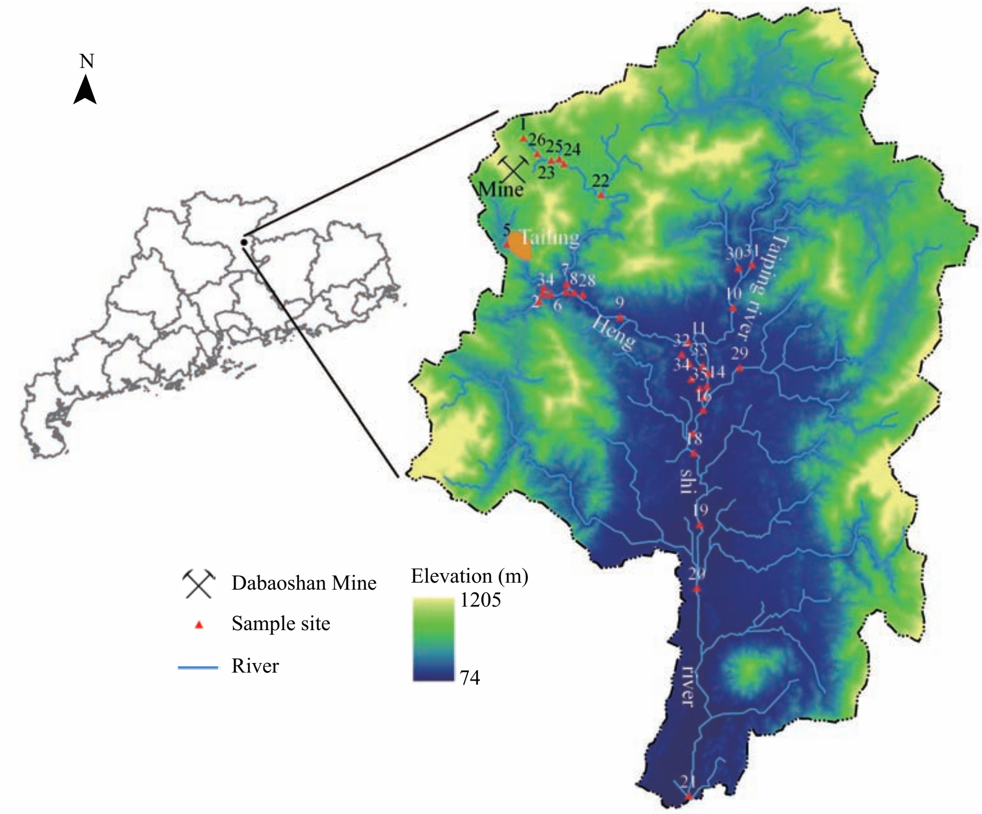

Fig. 1 Location and sample station map of the Dabaoshan Mine.

The Dabaoshan Mine belongs in the metallogenic province of polymetallic sulfide-pyrites in the north of Guangdong. The metallogenic province consists of western Guangxi, southern Hunan, and northern Guangdong. Several deep fractures pass through the area, and large-sized and medium-sized deposits are scattered in the fractures, and Dabaoshan Mine is one of the deposits. Iron, copper, zinc and lead are large-sized deposits in the mine and sulfur, tungsten and molybdenum are potentially available for industrial utilization.

The Dabaoshan Mountain is a huge intrusion of granitic rock. A volcanic eruption occurred in the Devonian period and dacite tuff and tuffaceous shale were widely spread in the ore belts. The deposit belongs to the class of volcano-sedimentary formations and was formed about the middle-early Devonian period.

1.2 Sample collection and preparation

Thirty five water samples in the vicinity of the Dabaoshan Mine were collected in June, 2009. The waters were classified into two groups based on both their hydrodynamic relationships and geological conditions. The first is affected water, which received the AMD directly, and the second is unaffected water, which was not influenced by AMD and is regarded as background water. All sample sites are shown in Fig. 1. Locations were established using a GARMIN global positioning system (GPS).

Nine sediments were collected during the water sampling period. Sediments included waste dump sediment (site 1), tailings dam sediment (site 5) and streambed sediment. Sediment sample locations were co-located with surface water sample sites. Streambed sediments were sampled along the Hengshi River. Site 18, the most distant collection point of sediment samples, was about 20 km away from the tailings dam (Fig. 1). At each sampling site, the top layer sediment (10 cm) was collected using a grab sampler, and a composite sample was formed by the mixing of 5 grab samples within 10 m^2 to represent each sampling site.

At each water sampling location, three sub-samples were collected across the river to form a composite sample to represent each sampling location. Water samples were filtered through 0.45 μm cellulose filters *in situ*, and the following were added: (1) supra pure HCl for iron speciation analysis; (2) supra pure HNO_3 to keep pH < 2 for heavy metal and other trace element analyses; and (3) no additional treatment for analyses of major anions. Water samples were stored in high-density polyethylene bottles in an icebox. Sediment samples were stored in dark bottles in the icebox. All the samples were transported to the laboratory within 12 hr. Water samples were stored at 4°C before analysis, and sediment samples were freeze-dried immediately.

1.3 Analysis procedures and methods

Temperature, pH, electrical conductivity (EC), oxidation-reduction potential (ORP), and total dissolved solids (TDS) were measured *in situ* with portable instruments (Orion 4-star, Thermo Scientific, USA).

Dissolved ion concentrations were measured using conventional methods. The major anions Cl^-, and SO_4^{2-} were analyzed with a Metrohm 732 ion chromatograph (Switzerland). Alkalinity was measured by an acid-base titration method with 0.025 mol/L HCl solution at pH of 4.4–4.5, within 24 hr after the samples were collected. The accuracy and precision were tested through triplicate analyses on selected samples.

Total Fe and Fe^{2+} were measured with 1, 10-Phenanthroline spectrophotometrically. Fe^{2+} was analyzed by colorimetry at 510 nm with a Shimadzu UV2450 spectrophotometer (Japan). The detection limit was 0.1 mg/L.

Heavy metals and other trace element concentrations were measured with inductively coupled plasma-optical emission spectrometry (ICP-OES) (Optima 5300DV, Perkin Elmer, USA) (Cánovas et al., 2007). K, Na, Ca and Mg were analyzed by Atomic Absorption Spectrometry (AAS) (Z-5000, Hitachi, Japan). Total As was determined by atomic fluorescence spectrometry (AFS-820, Beijing Titan, China). The accuracy and precision of the analytical methods were verified against certified reference materials: GSB04-1767-2004 (heavy metal and trace elements), GSBZ50020-90 (major cation) and GSBZ50004-88 (arsenic). The percent recoveries of elements were between 80% and 110%. A triplicate analysis was performed to evaluate the precision.

Sediment samples were pulverized before analysis. Mineralogy was characterized by powder X-ray diffraction (XRD), field emission scanning electron microscopy (FE-SEM) and Fourier transform infrared (FT-IR). The XRD analysis was carried out with an X-ray diffractometer (D/Max 2200 VPC, RIGAKU, Japan). The X-ray diffractometer was fitted with a 1.2 kW Cu $K\alpha$ X-ray source. Diffractograms were collected in step-scan mode (0.02°) in 2θ range of 3–80°. Patterns were interpreted with the aid of Scintag and MDI applications JADE search/match software and compared with reference patterns in the powder diffraction file (ICDD, 2002). The morphology of the secondary minerals was observed using FESEM (Quanta 400F, FEI/OXFORD/HKL, Dutch). The FT-IR spectra of the sediments were collected by the KBr pellet technique, and the spectra were collected in transmission mode in the 4000–400 cm^{-1} range with a spectral resolution of 4 cm^{-1}. The measurements were carried out on a FT-IR spectrometer (Nicolet iS10, Thermo Scientific, USA).

The classical 5-step Tessier sequential extraction procedure was used in this study (Table 1) (Tessier et al., 1979). The sequential extractions were performed in triplicate on 0.2 g of dried sediment. The reagents used during the extraction procedure were analysis grade and were prepared with Milli-Q water. Following each step, except for the residual, the extraction solutions were centrifuged at 5000 r/min for 30 min. The extraction solutions were filtered into sample vials and stored at 4°C before analysis. Heavy metals were measured by ICP-OES.

The PHREEQC geochemical modeling software package (v.2.15, February 5, 2008) (Parkhurst and Appelo, 1999) with wateq4f.dat was applied for the calculation

Table 1 Sequential extraction procedure used in this study*

Fraction	Extractant (dilution)	Procedure
Exchangeable fraction	1 mol/L $MgCl_2$ (pH = 7)	Continuous shaking for 2 hr at room temperature
Adsorbed carbonates	1 mol/L NaOAc (pH = 5)	Continuous shaking for 3 hr at room temperature
Fe-Mn oxides	0.04 mol/L NH_2OH-HCl	Heat in water bath 96°C for 6 hr
Organic matter	0.04 mol/L HNO_3-H_2O_2 and 3.2 mol/L NH_4OAc	30% H_2O_2 added twice to samples with 0.04 mol/L HNO_3 shaking in water bath 85°C for 3 hr, cool to room temperature, then added 3.2 mol/L NH_4OAc for 30 min
Residual	HCl-HNO_3-$HClO_4$	Sample digested with HCl, HNO_3 and $HClO_4$ in a microwave digester

* Tessier et al., 1979.

of saturation indices (SI), activities and theoretical pE (Eh) values based on the Fe^{2+}/Fe^{3+} redox couple. The thermodynamic database of schwertmannite ($\log k = 18.00 \pm 2.50$) was enlarged with the data from Bigham et al. (1996b).

2 Results and discussions

2.1 Chemical characteristics of water

The characteristics of surface water are shown in Table 2. High concentrations of TDS, SO_4^{2-}, Cu and Zn, with low Pb, Cd and As were the main characteristics of the affected water. The results were similar to prior studies (Allen et al., 1996; Kim and Chon, 2001; Sánchez-España et al., 2005; Wu et al., 2009).

The average concentration of HCO_3^- (44.06 mg/L) in affected water was significantly lower than that in unaffected water (71.75 mg/L) in the study area. The higher HCO_3^- samples were in the area adjacent to the karst strata, implying that carbonate rock dissolution was the main source of HCO_3^-.

The concentrations of major ions, HCO_3^-, SO_4^{2-}, Cl^-, Ca^{2+}, Mg^{2+}, Na^+ and K^+ fluctuated in affected water. All median values were higher than average values. The data distribution of the samples showed that the concentrations of these ions changed systematically with distance from the AMD source.

Piper diagrams are widely used for classifying hydrogeochemical types of water by major ion analysis (Halima et al., 2009). The content of major ions plotted on a Piper diagram showed obvious variation, especially for anion content. The dominant cation, Ca^{2+}, was abundant in both affected and unaffected water (Fig. 2).

The unaffected water samples were of the Ca-HCO_3 type. However, the samples collected from affected water were the Ca-SO_4 type. This reveals that the affected water received more SO_4^{2-} from the mine tailing.

2.2 pH, electrical conductivity (EC) and Eh

Generally, pH is the main factor influencing the chemical processes of AMD. The variations of chemical components in the affected and unaffected water were related to the pH. The highest pH value (7.09) was measured in unaffected water, and the lowest pH value (2.59) was detected in affected water (Table 2). In the study area, the pH values increased downstream of the Hengshi River, especially as an unaffected river flowed into the affected river. For

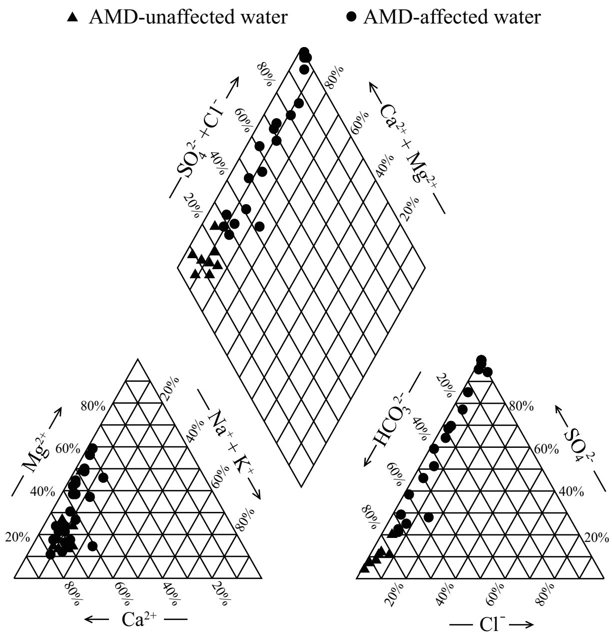

Fig. 2 Piper diagram showing the chemical composition of water samples in the study area.

example, pH increased substantially from 3.57 to 6.61 at Shangba village below the confluence of the unaffected river, the Taiping River, flowing into the Hengshi River. Lee and Kim (2008) observed a similar result.

The higher EC values in affected water revealed that more minerals were dissolved in affected water than in unaffected water. As shown in Fig. 3, the Ca^{2+}, Mg^{2+} and SO_4^{2-} concentrations have good correlations with EC (R^2 0.84, 0.94, and 0.93, respectively) indicating that EC might be used as an indicator of the contamination degree in AMD-affected water.

Water Eh is affected by several factors, such as dissolved oxygen, iron, chromium and manganese. However, the oxidation/reduction system of AMD is directly related to the oxidation of Fe^{2+} (Sánchez-España et al., 2005). The calculated pE values based on the concentrations of Fe^{2+} and Fe^{3+} were well correlated ($R^2 = 0.85$, $n = 17$) with *in situ* measured Eh values (Fig. 4), which means the redox potential of the AMD was governed by Fe ions.

2.3 Aluminum and iron

The average total Fe and Al^{3+} concentrations in affected water (12.95 mg/L and 13.07 mg/L, respectively) were much higher than those in unaffected water (0.16 mg/L and 0.1 mg/L, respectively). The Fe concentration was

Table 2 Statistical data for the geochemical parameters of the waters of Dabaoshan Mine in Guangdong, China

	Affected water (n = 27)				Unaffected water (n = 8)			
	Max	Min	Mean	Median	Max	Min	Mean	Median
pH	7.03	2.59	5.13	5.52	7.09	6.06	6.55	6.52
Eh (mV)	691.80	283.40	480.82	391.85	520.30	275.30	352.29	323.40
EC (μS/cm)	3090.00	25.35	698.28	342.50	596.00	40.30	194.50	111.40
TDS (mg/L)	1513.00	12.00	342.15	167.50	292.00	20.00	95.33	55.00
Cl^- (mg/L)	13.96	0.19	1.90	0.85	2.15	0.19	0.82	0.47
SO_4^{2-} (mg/L)	2108.00	2.89	295.37	77.97	19.28	2.18	6.58	4.61
HCO_3^- (mg/L)	130.61	3.06	44.06	26.62	308.04	21.26	71.75	45.10
K^+ (mg/L)	24.27	0.17	3.58	1.65	4.50	0.24	1.33	1.22
Na^+ (mg/L)	9.27	0.13	2.30	1.32	7.29	0.34	1.83	1.33
Ca^{2+} (mg/L)	490.00	0.66	67.59	35.61	78.42	5.13	19.26	8.97
Mg^{2+} (mg/L)	201.60	0.46	35.81	8.74	12.00	1.07	3.17	1.88
Cu^{2+} (mg/L)	7.67	0	1.74	0.29	0.01	0	0	0
Pb^{2+} (mg/L)	0.70	0.02	0.28	0.19	bd	bd	bd	bd
Cd^{2+} (mg/L)	0.25	0	0.09	0.07	bd	bd	bd	bd
Zn^{2+} (mg/L)	34.64	0	6.85	1.30	0.76	0.02	0.16	0.05
Total Fe (mg/L)	115.64	0.02	12.95	2.54	0.40	0.01	0.16	0.09
Fe^{2+} (mg/L)	68.62	0.01	6.21	1.17	0.14	0.01	0.07	0.07
Al^{3+} (mg/L)	62.61	0	13.07	2.51	0.19	0.03	0.10	0.09
Total As (mg/L)	0.03	0	0.01	0.01	0.02	0	0.01	0
Mn^{2+} (mg/L)	29.32	0	7.01	2.23	0.03	0	0.02	0.02
Sr^{2+} (mg/L)	0.43	0	0.08	0.06	0.16	0.01	0.04	0.02

TDS: total dissolved solid; bd: below detection limits.
Affected water sample were collected from sites 1, 2, 4–9, 11–23, 25, 26, 28, 32, 33 and 35; unaffected water sample were collected from sites 3, 10, 24, 27, 29-31 and 34.

positively related with the Al concentration (R^2 = 0.86, n = 27) in affected water, suggesting that Fe and Al in affected water originated from the minerals of the Dabaoshan Mine.

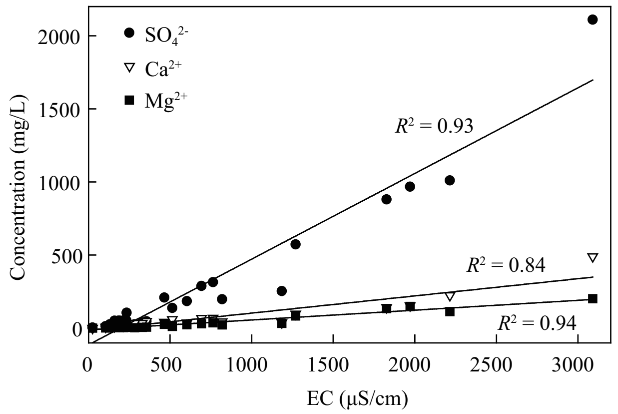

Fig. 3 Correlation plots of electrical conductivity (EC) vs. Ca^{2+}, Mg^{2+} and SO_4^{2-} concentration in the affected water of Dabaoshan Mine.

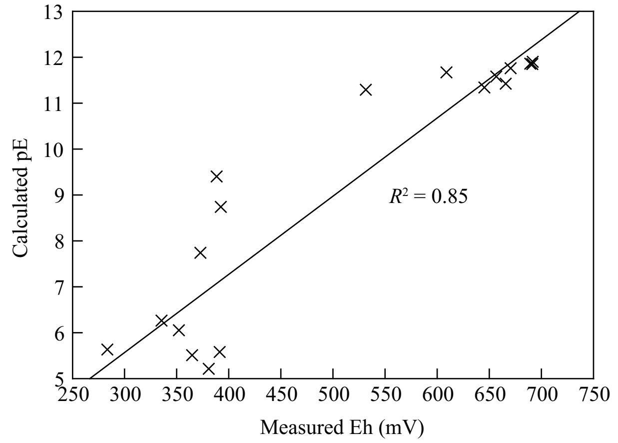

Fig. 4 Correlations between measured Eh and calculated pE. The measured Eh values were obtained on-site, whereas the calculated pE were computed with PHREEQC v. 2.15, by introducing measured Fe^{2+} and Fe^{3+} concentrations.

Fe exists as different species at different pH. Figure 5 shows that the concentration of Fe^{3+} in affected water decreases with rising pH, and the solubility of goethite and ferrihydrite have similar tendencies. The Fe^{3+} concentrations of all samples were higher than the solubility line of goethite at all pH, but below the solubility line of ferrihydrite at pH < 4.5, and above the line at pH > 4.5. This means that the deposition of Fe in affected water was controlled by pH.

Schwertmannite (ideal formula: $Fe_8O_8(OH)_6SO_4$) proved to be very important for iron precipitation in AMD (Bigham et al., 1996a; Eskandarpour et al., 2008; Sánchez-España et al., 2005, 2006, 2007, 2008; Yu et al., 1999). The calculation of saturation indices revealed that sediment suspensions were supersaturated with

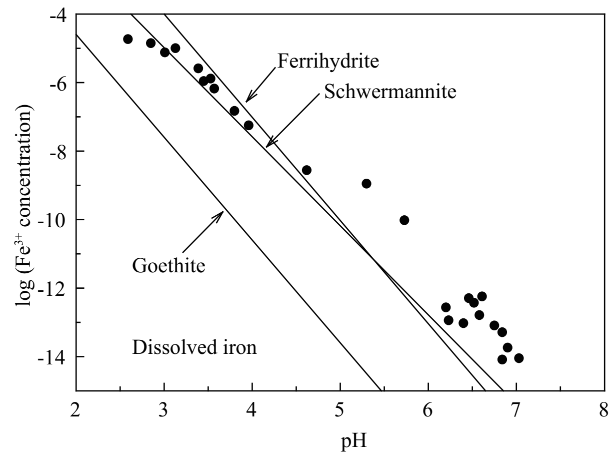

Fig. 5 Logarithm of Fe^{3+} activity vs. pH of the affected water of the Dabaoshan Mine with goethite, ferrihydrite and schwertmannite solubility lines (Bigham et al., 1996b).

respect to goethite and schwertmannite; the waters are undersaturated below pH 3.2, at saturation between pH 3.2 and 4, and supersaturated above pH 4 (Fig. 5). Thus, the precipitate of schwertmannite may govern the activities of Fe^{3+} ions above pH 4 and Fe ions could be rapidly removed from the AMD as Fe^{3+} oxyhydroxide precipitates with increasing pH.

2.4 Trace elements

Sediment is an important factor as AMD is discharged at mining sites. Sediment geology and mineralogy are helpful in understanding the environmental activities of heavy metals and trace elements in AMD.

Cadmium exists in sphalerite accompanied by Zn, and the geochemical characteristics of Cd are similar to Zn. The concentrations of Zn and Cd in affected water were well correlated (R^2 = 0.97, n = 27). Ullrich et al. (1999) and Shikazono et al. (2008) reported that Cd and Zn were always found together in nature and their concentrations were closely correlated. The correlations between Al and other metal ions are also significant, e.g. Al:Zn (R^2 = 0.98), Al:Cu (R^2 = 0.94), Al:Pb (R^2 = 0.97), Al:Cd (R^2 = 0.97) and Al:Mn (R^2 = 0.85). It is possible that these elements originated from the same minerals at the mine site.

Another significant geochemical characteristic is the association of potassium and strontium (R^2 = 0.90, n = 27) in affected water. It may be inferred from this correlation that strontium and potassium originated from the same minerals.

2.5 Mineralogy of AMD sediments

The most widespread feature of the study area is the ocher sediments on riverbanks affected by AMD. These sediments consist of Fe-phases precipitated from the Fe dissolved in AMD and coming from pyrite at the mine site. The minerals of AMD sediment have been well characterized in many mine areas all over the world by different techniques (SEM, XRD and FT-IR). The minerals consist of tiny particle size (from µm to nm in diameter), amorphous oxyhydroxides and oxyhydroxysulfates with fibrous to spherical appearance, such as schwertmannite and goethite.

Ocher sediments of Fe-minerals were found at the waste dumps (site 1), tailings dam (site 5) and river (sites 8, 9, 16 and 18) in the Dabaoshan Mine area. The secondary minerals are formed as the AMD leaches from the mine tips. Soil-free or loosely held modes can be observed in the entire system.

Schwertmannite is the dominant mineral at site 1 (waste dumps) as shown by XRD analysis (Fig. 6 line a), which due to the continuous injection and slow flow of AMD. Goethite and quartz with trace amounts of schwertmannite are present at sites 5 (tailings dam), 8, 9, 16 and site 18 (Fig. 6 line b) (Hengshi River). The presence of goethite together with trace schwertmannite indicates that schwertmannite is metastable with respect to goethite in these systems. The transformation of schwertmannite to goethite has been observed both under laboratory conditions (Acero et al., 2006; Bigham et al., 1996b; Jönsson et al., 2005; Kawano and Tomita, 2001) and under natural conditions (Asta et al., 2010; Gagliano et al., 2004; Kumpulainen et al., 2007; Pérez-López et al., 2011). The minerals changed in the tailings dam and riverbanks. This might be due to the warm weather in the study area and the fact that schwertmannite had enough time to be transformed into goethite. The transformation occurs via the overall reaction (Bigham et al., 1996b):

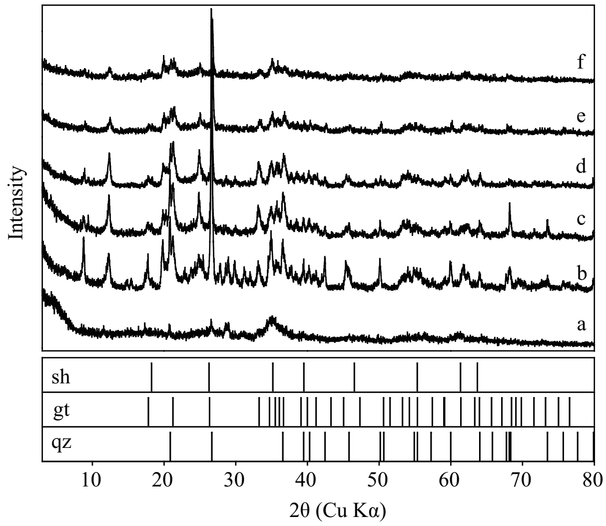

Fig. 6 X-ray powder diffraction pattern of precipitates from the waste dump (site 1 line a) and tailings dam (site 5, line b) and Hengshi creek; line c: site 8; line d: site 9; line e: site 16; line f: site 18. gt: goethite, sh: schwertmannite, qz: quartz.

$$Fe_8O_8(OH)_{5.5}(SO_4)_{1.25(s)} + 2.5H_2O_{(l)} = 8FeOOH_{(s)} + 2.5H^+_{(aq)} + 1.25SO_4^{2-}{}_{(aq)} \quad (3)$$

SEM analysis of site 1 showed that schwertmannite formed spherical particles of 1–2 µm diameter (Fig. 7) that were associated in larger aggregates. Both spherical and fibrous particles observed at site 5 indicated that schwertmannite and goethite coexisted. Characteristic filamentous features were observed for the schwertmannite spherical particles in site 1. Spherical phases were present at sites 8 and 9. The SEM revealed a low crystalline phase at sites 16 and 18 and ultrafine particles adhered to the grains.

FT-IR has been widely used to analyze the minerals generated from AMD. The studies have mainly focused on the minerals generated under conditions of different pH (Boily et al., 2010; Jönsson et al., 2005; Peak et al., 1999; Zhang and Peak, 2007), temperature (Boily et al., 2010) and depth (Gagliano et al., 2004). However, few have studied the FT-IR spectra of minerals generated at varying distance from the mine tailing under natural conditions.

The FT-IR analysis of site 1 exhibited the characteristic OH deformations (700 and 850 cm^{-1}) (Fig. 8a) and stretches (3400 cm^{-1}) (not shown) of schwertmannite, which were consistent with the XRD and SEM analysis. The ν_{so} modes of schwertmannite consisted of a broad triply degenerate ν_3 band at 1128 cm^{-1} with shoulders at 1040 and 1205 cm^{-1}, a ν_1 fundamental band of the SO_4^{2-} stretch at 980 cm^{-1}, and a ν_4 bending band at 610 cm^{-1}. The spectra implied that bidentate sulfate complexes of C_{2v} symmetry occur on the schwertmannite surface

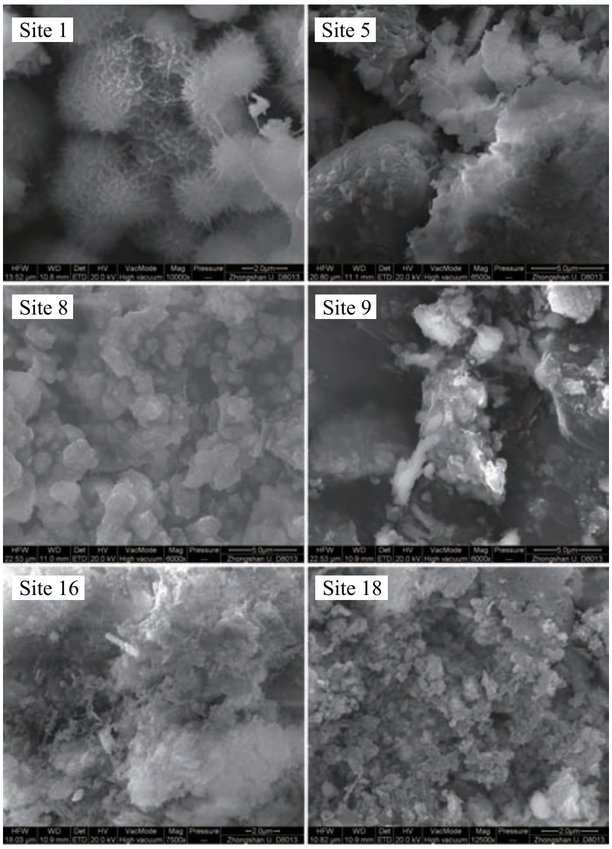

Fig. 7 Scanning electron microscopy images of precipitates from different sites.

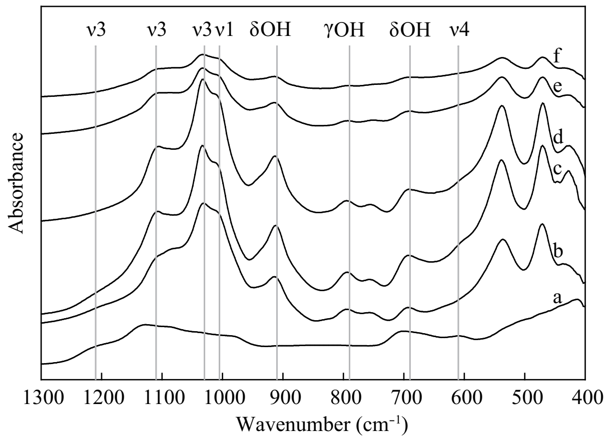

Fig. 8 FT-IR spectra of precipitates from the waste dump (site 1, line a) and tailings dam (site 5, line b) and Hengshi creek: (line c) site 8; (line d) site 9; (line e) site 16; and (line f) site 18.

(Nakamoto, 2009; Peretyazhko et al., 2009). The spectra of the sediment samples collected from the tailings dam (site 5) and Hengshi River (sites 8, 9, 16 and 18) were different from that of the waste dumps (site 1). The v_1 band becomes active at 1005 cm^{-1}, while the v_3 band split into 1106, 1032, and 1208 cm^{-1} at sites 5 and 8 (Fig. 8 line b, c). The 1208 cm^{-1} band vanished at sites 9, 16, and 18 (Fig. 8 line d–f), indicating that the bidentate C_{2v} complexes were transformed to monodentate complexes of C_{3v} symmetry on the mineral surface downstream in the river. Peretyazhko et al. (2009) reported a conversion of bidentate- to monodentate-bound sulfate complexes accompanied by sulfate desorption in AMD minerals. The formation of goethite and other minerals, as influenced by the presence of co-precipitated silicate, showed broad FT-IR bands at 538 and 469 cm^{-1} (silicate bending region) (Nakamoto, 2009; Vempati and Loeppert, 1989). The quartz present in the streambed sediments was confirmed by XRD analysis, as shown in Fig. 6.

The results indicated that fresh sediments at site 1 (waste dumps) were composed of metastable schwertmannite. The schwertmannite in sediments of the Hengshi River gradually transformed at distances over short time scales into goethite, and the quantities of goethite increased with the distance away from the tailing.

2.6 Sequential extraction of sediment

The newer revised sequential extraction methods (Caraballo et al., 2009; Dold, 2003) used in sulfide wastes and in acid mine water passive remediation systems were developed after Tessier et al. (1979) introduced the five step sequential extraction method. To compare our results to other studies, we selected the classical Tessier 5-step sequential extraction method in this article. Five phases were extracted from the sediment samples (Fig. 9): exchangeable, carbonates, Fe-Mn oxides, organic matter and residual. The exchangeable phase contained the heavy metals adsorbed on the major constituents of the sediment. The carbonates fraction showed that some heavy metals were associated with sediment carbonate. This fraction was liberated with a pH change. The Fe-Mn oxides phase was cemented or coated on the particles. These phases were unstable under anoxic conditions. The organic matter phase consists of heavy metals bound to various organic matter forms. The residual fraction consists of the heavy metals held within the mineral crystal structures (Ranville et al., 2004; Tessier et al., 1979). Carbonates and Fe-Mn oxide extractions were considered chemically mobile. These phases could liberate heavy metals to the environment as the geochemical conditions change (Ranville et al., 2004).

Heavy metals show different affinities within the sequential extraction phases. Pb, Zn and Cu have a high affinity for absorption on Fe-hydroxides (Lee et al., 2002; Lottermoser et al., 1999; Ranville et al., 2004). Cu in the bioavailable phase (organic matter) increased after the AMD confluence with other creeks (Ranville et al., 2004), and the mineral form was $Cu_2(OH_2)CO_3$ as predicted by Chapman et al. (1983). Cd was primarily found in the silicate (residual) and Fe oxide phases (Ranville et al., 2004). The sequential extraction results are shown in Fig. 9. The exchangeable fraction of Cu, Zn, Pb and Cd decreased downstream in the river. The carbonate phases of Cu, Zn, Pb and Cd increased further away from the mine site. The Fe-Mn oxide phases of Zn, Cd and Pb increased, while Cu decreased except at site 9, downstream in the river. Organic matter phases of Zn and Cd decreased, but there was an increase in Cu downstream. The organic matter phase of Pb increased before site 9 and then decreased. The residual phase of the four elements dominated in the Hengshi river sediments. Except for the residual phase, the other four phases were different for Cu, Zn, Pb and Cd. The Fe-Mn

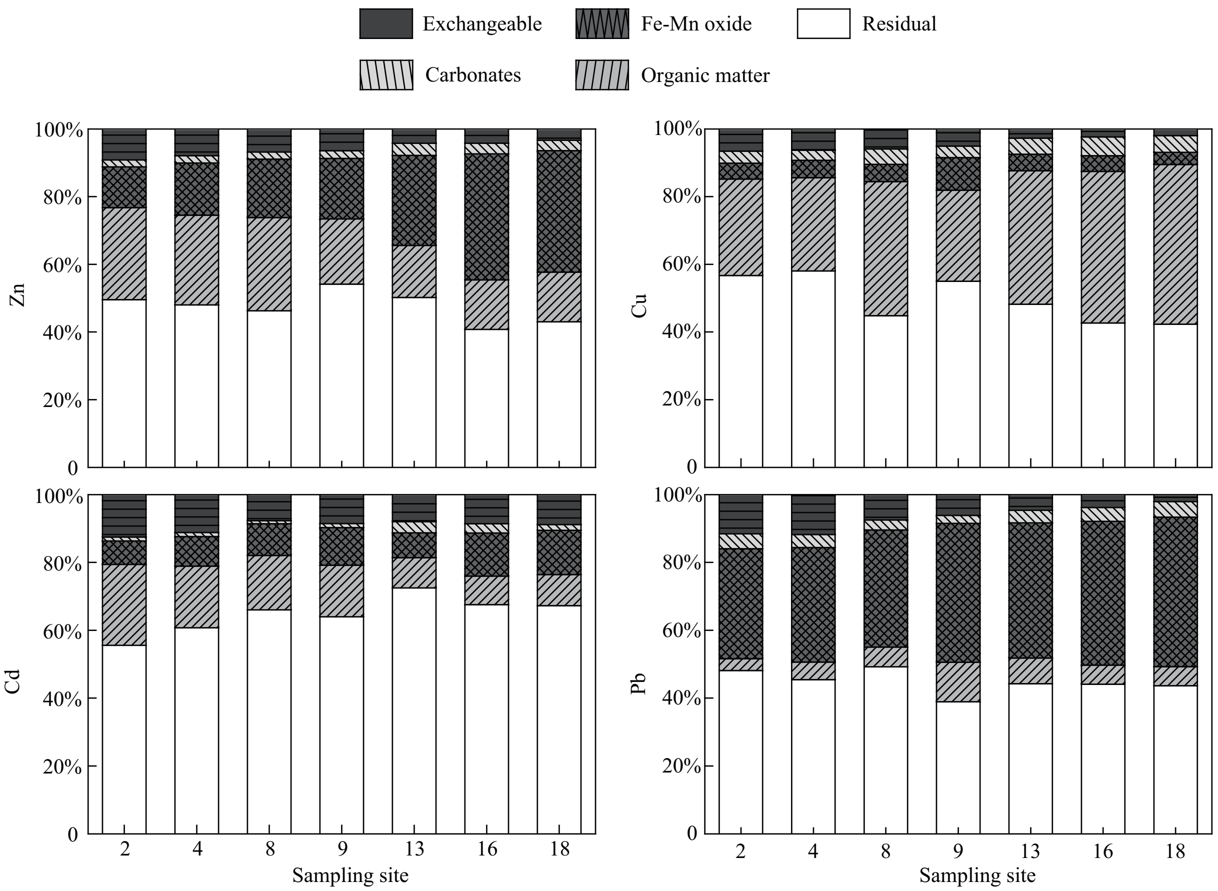

Fig. 9 Sequential extractions of the sediments of Hengshi River.

oxide phase was dominant for Pb, and carbonate was the major phase for Cu. The carbonate phase was dominant at site 2 (upstream) while the Fe-Mn was the main oxide phase at site 18 (downstream) for Zn.

2.7 Attenuation of heavy metals in AMD

AMD systems are complex and a combination of processes exists. Heavy metals in AMD can be removed by adsorption, deposition, co-precipitation and bioremediation (Neculita et al., 2007). The adsorption, deposition and co-precipitation are physicochemical processes in the systems, and the pH value affects their removal efficiency of heavy metals. As the unpolluted river inflow enters the AMD-affected river, the pH, ORP, TDS and other indexes of the systems would be changed. Moreover, the unpolluted river would dilute the systems and accelerate the reactions in the systems.

Attenuation of heavy metals in AMD has been proven by the variation in content of heavy metals and SO_4^{2-}. Heavy metal and SO_4^{2-} concentrations in the Hengshi River were above background values when the AMD flowed into the river, and decreased after the Taiping River inflow. At the confluence, the pH increased (from 3.57 to 6.61), and EC (from 693 to 105 μS/cm), ORP (from 665.8 to 283.4 mV), HCO_3^- (from 0 to 20.91 mg/L), SO_4^{2-} (from 287.25 to 10.83 mg/L) and heavy metals (from 1.58 to 0.01 mg/L for Cu, from 0.13 mg/L to below detection limits for Pb, from 0.04 mg/L to below detection limits for Cd, from 8.05 to 0.08 mg/L for Zn and from 0.01 mg/L to below detection limits for As) decreased. The variation in concentrations of heavy metals and other ions in the Hengshi River may be explained by the secondary Fe or Al-oxyhydroxide minerals' selective adsorption. Removal of heavy metals by adsorption onto these minerals has been established under both field and laboratory conditions. Several studies revealed that Cu, Zn and Pb are adsorbed on the Fe hydroxide surface (Chapman et al., 1983; Dzombak and Morel, 1990; Johnson, 1986). Al hydroxides or hydroxysulfates can adsorb Pb, Cu, Zn and Ni (Munk et al., 2002). The maximum sorption of As occurred at pH 3–7, and declined with the increase of pH (Adriano, 2001). Fukushi et al. (2003) reported that As was rapidly scavenged from drainage water in abandoned arsenic mine dumps by sorption on hydrous iron oxides. Fe oxyhydroxide precipitation played an important role in the removal of heavy metals by adsorption and co-precipitation (Benjamin, 1983; Stumm and Sulzberger, 1992).

AMD could be neutralized by the dissolution of carbonate minerals, and the mine tailing belongs to the carbonate-type in the study area. The AMD of the Dabaoshan mine is initially strong acidic because H^+ ions liberated by sulfide oxidation are not consumed by the dissolution of carbonate minerals immediately. Limestone is widespread in the study area. When the AMD moves away from the mine tailing, the dissolution of carbonate minerals takes place, and the acidity produced by the sulfide minerals is buffered by the carbonate minerals. This results in increase of the pH and decrease of heavy metal concentrations in water, and transformation of secondary minerals in sediment.

Due to the natural attenuation processes, such as secondary minerals adsorption and co-precipitation, carbonate minerals buffering, and unaffected water dilution, the hydrogeochemical characteristics of the affected water and the unaffected water become similar downstream in the Hengshi River.

3 Conclusions

The chemical characteristics of affected water in the vicinity of the Dabaoshan Mine are controlled by sulfide minerals in spite of the AMD belonging to the carbonate-type. AMD is characterized by low pH (5.13) and high concentrations of heavy metals (1.74 mg/L Cu, 0.28 mg/L Pb, 0.09 mg/L Cd and 6.85 mg/L Zn) and SO_4^{2-} (295.37 mg/L). In affected water, Ca^{2+} and SO_4^{2-} were the major ions, whereas Ca^{2+} and HCO_3^- dominated in unaffected water.

The good correlation (R^2 = 0.85, n = 17) between calculated pE and *in situ* measured Eh, suggests that the Fe^{2+}/Fe^{3+} couple determined the redox potential of the affected water. The pH increased, while the heavy metals and SO_4^{2-} concentrations decreased downstream, especially at the unaffected river confluence. SEM, XRD, FT-IR, sequential extraction experiment and PHREEQC simulation results showed that secondary Fe minerals precipitated in the affected water, which was confirmed by the observation of ocher precipitations in the field. Schwertmannite was the major mineral at the waste dump, while goethite was dominant at the tailings dam and riverbank. The bidentate complexes of C_{2v} symmetry transformed to monodentate complexes of C_{3v} symmetry in the sulfate radical of secondary minerals, downstream. Fe-Mn oxide phases of Zn, Cd and Pb in sediments increased downstream, however, the organic matter complexes of Cu in sediments increased further away from the AMD sources.

Heavy metal attenuations are very complex processes in AMD. The heavy metal adsorption or co-precipitation on other minerals (such as: Al or Mn minerals) requires further study in this region. Moreover, a detailed research study of the mineral transformations should also be initiated.

Acknowledgments

This study was supported by the Guangdong Provincial Natural Science Foundation (No. 06202438) and the Research Funds of the Guangxi Key Laboratory of Environmental Engineering, Protection and Assessment (No. GuiKeNeng 0801Z020).

References

Acero P, Ayora C, Torrentó C, Nieto J M, 2006. The behavior of trace elements during schwertmannite precipitation and subsequent transformation into goethite and jarosite. *Geochimica et Cosmochimica Acta*, 70(16): 4130–4139.

Adriano D C, 2001. Trace Elements in Terrestrial Environments: Biogeochemistry, Bioavailability, and Risks of Metals. Springer Verlag, New York.

Allen S K, Allen J M, Lucas S, 1996. Concentrations of contaminants in surface water samples collected in west-central Indiana impacted by acidic mine drainage. *Environmental Geology*, 27(1): 34–37.

Asta M P, Ayora C, Román-Ross G, Cama J, Acero P, Gault A G et al., 2010. Natural attenuation of arsenic in the Tinto Santa Rosa acid stream (Iberian Pyritic Belt, SW Spain): The role of iron precipitates. *Chemical Geology*, 271(1-2): 1–12.

Bao Q S, Lu C Y, Song H, Wang M, Ling W H, Chen W Q et al., 2009. Behavioural development of school-aged children who live around a multi-metal sulphide mine in Guangdong province, China: a cross-sectional study. *BMC Public Health*, 9(1): 217.

Benjamin M M, 1983. Adsorption and surface precipitation of metals on amorphous iron oxyhydroxide. *Environmental Science & Technology*, 17(11): 686–692.

Bigham J M, Schwertmann U, Pfab G, 1996a. Influence of pH on mineral speciation in a bioreactor simulating acid mine drainage. *Applied Geochemistry*, 11(6): 845–849.

Bigham J M, Schwertmann U, Traina S J, Winland R L, Wolf M, 1996b. Schwertmannite and the chemical modeling of iron in acid sulfate waters. *Geochimica et Cosmochimica Acta*, 60(12): 2111–2121.

Boily J F, Gassman P L, Peretyazhko T, Szanyi J, Zachara J M, 2010. FTIR spectral components of schwertmannite. *Environmental Science & Technology*, 44(4): 1185–1190.

Cánovas C R, Olías M, Nieto J M, Sarmiento A M, Cerón J C, 2007. Hydrogeochemical characteristics of the Tinto and Odiel Rivers (SW Spain). Factors controlling metal contents. *Science of the Total Environment*, 373(1): 363–382.

Caraballo M A, Rotting T S, Nieto J M, Ayora C, 2009. Sequential extraction and DXRD applicability to poorly crystalline Fe- and Al-phase characterization from an acid mine water passive remediation system. *American Mineralogist*, 94(7): 1029–1038.

Chapman B M, Jones D R, Jung R F, 1983. Processes controlling metal ion attenuation in acid mine drainage streams. *Geochimica et Cosmochimica Acta*, 47(11): 1957–1973.

Chen A, Lin C, Lu W, Wu Y, Ma Y, Li J et al., 2007. Well water contaminated by acidic mine water from the Dabaoshan Mine, South China: Chemistry and toxicity. *Chemosphere*, 70(2): 248–255.

Dold B, 2003. Speciation of the most soluble phases in a sequential extraction procedure adapted for geochemical studies of copper sulfide mine waste. *Journal of Geochemical Exploration*, 80(1): 55–68.

Dzombak D A, Morel F M M, 1990. Surface Complexation Modeling: Hydrous Ferric Oxide. Wiley-Interscience, New York.

Eskandarpour A, Onyango M S, Ochieng A, Asai S, 2008. Removal of fluoride ions from aqueous solution at low pH using schwertmannite. *Journal of Hazardous Materials*, 152(2): 571–579.

Fukushi K, Sasaki M, Sato T, Yanase N, Amano H, Ikeda H, 2003. A natural attenuation of arsenic in drainage from an abandoned arsenic mine dump. *Applied Geochemistry*, 18(8): 1267–1278.

Gagliano W B, Brill M R, Bigham J M, Jones F S, Traina S J, 2004. Chemistry and mineralogy of ochreous sediments in a constructed mine drainage wetland. *Geochimica et*

Cosmochimica Acta, 68(9): 2119–2128.

Ge C, Han F, 1987. Geological and Geochemical Features of Exhalativie-sedimentary Mineralization of the Dabaoshan Deposit in Guangdong Province. Beijing Science and Technology Press, Beijing.

Halima M A, Majumder R K, Nessa S A, Hiroshiro Y, Uddin M J, Shimada J et al., 2009. Hydrogeochemistry and arsenic contamination of groundwater in the Ganges Delta Plain, Bangladesh. *Journal of Hazardous Materials*, 164(2-3): 1335–1345.

Holmström H, Ljungberg J, Öhlander B, 1999. Role of carbonates in mitigation of metal release from mining waste. Evidence from humidity cells tests. *Environmental Geology*, 37(4): 267–280.

ICDD, 2002. Powder diffraction file release 2002, PDF-2: International Centre for Diffraction Data, Newton Square, Pa. http://www.icdd.com.

Jönsson J, Persson P, Sjöberg S, Lövgren L, 2005. Schwertmannite precipitated from acid mine drainage: phase transformation, sulphate release and surface properties. *Applied Geochemistry*, 20(1): 179–191.

Johnson C A, 1986. The regulation of trace element concentrations in river and estuarine waters contaminated with acid mine drainage: The adsorption of Cu and Zn on amorphous Fe oxyhydroxides. *Geochimica et Cosmochimica Acta*, 50(11): 2433–2438.

Kawano M, Tomita K, 2001. Geochemical modeling of bacterially induced mineralization of schwertmannite and jarosite in sulfuric acid spring water. *American Mineralogist*, 86(10): 1156–1165.

Kim J Y, Chon H T, 2001. Pollution of a water course impacted by acid mine drainage in the Imgok creek of the Gangreung coal field, Korea. *Applied Geochemistry*, 16(11-12): 1387–1396.

Kumpulainen S, Carlson L, Räisänen M L, 2007. Seasonal variations of ochreous precipitates in mine effluents in Finland. *Applied Geochemistry*, 22(4): 760–777.

Lee G, Bigham J M, Faure G, 2002. Removal of trace metals by coprecipitation with Fe, Al and Mn from natural waters contaminated with acid mine drainage in the Ducktown Mining District, Tennessee. *Applied Geochemistry*, 17(5): 569–581.

Lee J E, Kim Y, 2008. A quantitative estimation of the factors affecting pH changes using simple geochemical data from acid mine drainage. *Environmental Geology*, 55(1): 65–75.

Li Y T, Becquer T, Dai J, Quantin C, Benedetti M F, 2009. Ion activity and distribution of heavy metals in acid mine drainage polluted subtropical soils. *Environmental Pollution*, 157(4): 1249–1257.

Lin C, Tong X, Lu W, Yan L, Wu Y, Nie C et al., 2005a. Environmental impacts of surface mining on mined lands, affected streams and agricultural lands in the Dabaoshan Mine region, southern china. *Land Degradation & Development*, 16(5): 463–474.

Lin C, Lu W, Wu Y, 2005b. Agricultural soils irrigated with acidic mine water: acidity, heavy metals, and crop contamination. *Australian Journal of Soil Research*, 43(7): 819–826.

Lin C, Wu Y, Lu W, Chen A, Liu Y, 2007. Water chemistry and ecotoxicity of an acid mine drainage-affected stream in subtropical China during a major flood event. *Journal of Hazardous Materials*, 142(1-2): 199–207.

Liu Y, Lin C, Ma Y, Lu W, Wu Y, Huang S et al., 2009. Toxic effects of two acid sulfate soils from the Dabaoshan Mine on *Corymbia citriodora var. variegata* and *Daphnia carinata*. *Journal of Hazardous Materials*, 166(2-3): 1162–1168.

Lottermoser B G, Ashley P M, Lawie D C, 1999. Environmental geochemistry of the Gulf Creek copper mine area, north-eastern New South Wales, Australia. *Environmental Geology*, 39(1): 61–74.

Morin K A, Hutt N M, 1997. Environmental Geochemistry of Minesite Drainage: Practical Theory and Case Studies. MDAG Publishing, Vancouver, Canada.

Munk L, Faure G, Pride D E, Bigham J M, 2002. Sorption of trace metals to an aluminum precipitate in a stream receiving acid rock-drainage; Snake River, Summit County, Colorado. *Applied Geochemistry*, 17(4): 421–430.

Mylona E, Xenidis A, Paspaliaris I, 2000. Inhibition of acid generation from sulphidic wastes by the addition of small amounts of limestone. *Minerals Engineering*, 13(10-11): 1161–1175.

Nakamoto K, 2009. Infrared and Raman Spectra of Inorganic and Coordination Compounds, Applications in Coordination, Organometallic, and Bioinorganic Chemistry. Wiley-Interscience.

Neculita C M, Zagury G J, Bussiere B, 2007. Passive treatment of acid mine drainage in bioreactors using sulfate-reducing bacteria. *Journal of Environmental Quality*, 36(1): 1–16.

Pérez-López R, Asta M P, Román-Ross G, Nieto J M, Ayora C, Tucoulou R, 2011. Synchrotron-based X-ray study of iron oxide transformations in terraces from the Tinto-Odiel river system: Influence on arsenic mobility. *Chemical Geology*, 280(3-4): 336–343.

Parkhurst D L, Appelo C A J, 1999. User's Guide to PHREEQC (Version 2)–A Computer Program for Speciation, Batch-reaction, One-dimensional Transport, and Inverse geochemical Calculations. Vol 99-4259. U.S. Geological Survey, Denver, Colorado.

Peak D, Ford R G, Sparks D L, 1999. An *in Situ* ATR-FTIR investigation of sulfate bonding mechanisms on goethite. *Journal of Colloid and Interface Science*, 218(1): 289–299.

Peretyazhko T, Zachara J M, Boily J F, Xia Y, Gassman P L, Arey B W et al., 2009. Mineralogical transformations controlling acid mine drainage chemistry. *Chemical Geology*, 262(3-4): 169–178.

Ranville M, Rough D, Flegal A R, 2004. Metal attenuation at the abandoned Spenceville copper mine. *Applied Geochemistry*, 19(5): 803–815.

Robbins E I, Cravotta C A, Savela C E, Nord G L Jr, 1999. Hydrobiogeochemical interactions in 'anoxic' limestone drains for neutralization of acidic mine drainage. *Fuel*, 78(2): 259–270.

Sánchez-España J, Pamo E L, Pastor E S, 2007. The oxidation of ferrous iron in acidic mine effluents from the Iberian Pyrite Belt (Odiel Basin, Huelva, Spain): Field and laboratory rates. *Journal of Geochemical Exploration*, 92(2-3): 120–132.

Sánchez-España J, Pamo E L, Pastor E S, Andrés J R, Rubí J A M, 2006. The removal of dissolved metals by hydroxysulphate precipitates during oxidation and neutralization of acid mine waters, Iberian Pyrite Belt. *Aquatic Geochemistry*, 12(3): 269–298.

Sánchez-España J, Pamo E L, Pastor E S, Ercilla M D, 2008. The acidic mine pit lakes of the Iberian Pyrite Belt: An approach to their physical limnology and hydrogeochemistry. *Applied Geochemistry*, 23(5): 1260–1287.

Sánchez-España J, Pamo E L, Santofimia E, Aduvire O, Reyes J, Barettino D, 2005. Acid mine drainage in the Iberian Pyrite Belt (Odiel river watershed, Huelva, SW Spain):

Geochemistry, mineralogy and environmental implications. *Applied Geochemistry*, 20(7): 1320–1356.

Shikazono N, Zakir H M, Sudo Y, 2008. Zinc contamination in river water and sediments at Taisyu Zn-Pb mine area, Tsushima Island, Japan. *Journal of Geochemical Exploration*, 98(3): 80–88.

Stumm W, Sulzberger B, 1992. The cycling of iron in natural environments: Considerations based on laboratory studies of heterogeneous redox processes. *Geochimica et Cosmochimica Acta*, 56(8): 3233–3257.

Sydnor M E W, Redente E F, 2002. Reclamation of high-elevation, acidic mine waste with organic amendments and topsoil. *Journal of Environmental Quality*, 31(5): 1528-1537.

Task B, 1989. Draft acid rock drainage technical guide - Volume 1. Prepared by Steffen Robertson and Kirsten (SRK), Vancouver, BC.

Tessier A, Campbell P G C, Bisson M, 1979. Sequential extraction procedure for the speciation of particulate trace metals. *Analytical Chemistry*, 51(7): 844–851.

Tordoff G M, Baker A J M, Willis A J, 2000. Current approaches to the revegetation and reclamation of metalliferous mine wastes. *Chemosphere*, 41(1-2): 219–228.

Ullrich S M, Ramsey M H, Helios-Rybicka E, 1999. Total and exchangeable concentrations of heavy metals in soils near Bytom, an area of Pb/Zn mining and smelting in Upper Silesia, Poland. *Applied Geochemistry*, 14(2): 187–196.

Vempati R K, Loeppert R H, 1989. Influence of structural and adsorbed Si on the transformation of synthetic ferrihydrite. *Clays and Clay Minerals*, 37(3): 273–279.

Wu P, Tang C Y, Liu C Q, Zhu L J, Pei T Q, Feng L J, 2009. Geochemical distribution and removal of As, Fe, Mn and Al in a surface water system affected by acid mine drainage at a coalfield in Southwestern China. *Environmental Geology*, 57(7): 1457–1467.

Yu J Y, Heo B, Choi I K, Cho J P, Chang H W, 1999. Apparent solubilities of schwertmannite and ferrihydrite in natural stream waters polluted by mine drainage. *Geochimica et Cosmochimica Acta*, 63(19-20): 3407–3416.

Zhang G Y, Peak D, 2007. Studies of Cd(II)-sulfate interactions at the goethite-water interface by ATR-FTIR spectroscopy. *Geochimica et Cosmochimica Acta*, 71(9): 2158–2169.

Zhou J M, Dang Z, Cai M F, Liu C Q, 2007. Soil heavy metal pollution around the Dabaoshan Mine, Guangdong Province, China. *Pedosphere*, 17(5): 588–594.

Zhou X, Xia B C, 2010. Defining and modeling the soil geochemical background of heavy metals from the Hengshi River watershed (southern China): Integrating EDA, stochastic simulation and magnetic parameters. *Journal of Hazardous Materials*, 180(1-3): 542–551.

Zhuang P, McBride M B, Xia H P, Li N Y, Lia Z A, 2009a. Health risk from heavy metals via consumption of food crops in the vicinity of Dabaoshan mine, South China. *Science of the Total Environment*, 407(5): 1551–1561.

Zhuang P, Zou B, Li N Y, Li Z A, 2009b. Heavy metal contamination in soils and food crops around Dabaoshan mine in Guangdong, China: implication for human health. *Environmental Geochemistry and Health*, 31(6): 707–715.

JOURNAL OF ENVIRONMENTAL SCIENCES

Journal of Environmental Sciences (Established in 1989)
Vol. 24 No. 6 2012

Supervised by	Chinese Academy of Sciences	**Published by**	Science Press, Beijing, China
Sponsored by	Research Center for Eco-Environmental Sciences, Chinese Academy of Sciences		Elsevier Limited, The Netherlands
Edited by	Editorial Office of Journal of Environmental Sciences (JES) P. O. Box 2871, Beijing 100085, China Tel: 86-10-62920553; http://www.jesc.ac.cn E-mail: jesc@263.net, jesc@rcees.ac.cn	**Distributed by** Domestic	Science Press, 16 Donghuangchenggen North Street, Beijing 100717, China Local Post Offices through China
		Foreign	Elsevier Limited http://www.elsevier.com/locate/jes
Editor-in-chief	Hongxiao Tang	**Printed by**	Beijing Beilin Printing House, 100083, China

CN 11-2629/X **Domestic postcode: 2-580** **Domestic price per issue RMB ¥ 110.00**

ISSN 1001-0742